THE JOURNAL OF PHYSICAL CHEMISTRY Letters

ACS Editors' Choice

Letter

pubs.acs.org/JPCL

Terms of Use

Iron-Treated NiO as a Highly Transparent p-Type Protection Layer for Efficient Si-Based Photoanodes

Bastian Mei,[†,§] Anastasia A. Permyakova,[†,§] Rasmus Frydendal,[†,§] Dowon Bae,[†] Thomas Pedersen,[‡] Paolo Malacrida,[†] Ole Hansen,[‡] Ifan E. L. Stephens,[†] Peter C. K. Vesborg,[†] Brian Seger,[†] and Ib Chorkendorff*[,†]

[†]Department of Physics, Center for Individual Nanoparticle Functionality (CINF) and [‡]Department of Micro- and Nanotechnology, Technical University of Denmark, DK-2800 Kongens Lyngby, Denmark

Supporting Information

ABSTRACT: Sputter deposition of 50 nm thick NiO films on p^+−n-Si and subsequent treatment in an Fe-containing electrolyte yielded highly transparent photoanodes capable of water oxidation (OER) in alkaline media (1 M KOH) with high efficiency and stability. The Fe treatment of NiO thin films enabled Si-based photoanode assemblies to obtain a current density of 10 mA/cm^2 (requirement for >10% efficient devices) at 1.15 V versus RHE (reversible hydrogen electrode) under red-light (38.6 mW/cm^2) irradiation. Thus, the photoanodes were harvesting ∼80 mV of free energy (voltage), which places them among the best-performing Si-based photoanodes in alkaline media. The stability was proven by chronoamperometry at 1.3 V versus RHE for 300 h. Furthermore, measurements with electrochemical quartz crystal microbalances coupled with ICP-MS showed minor corrosion under dark operation. Extrapolation of the corrosion rate showed stability for more than 2000 days of continuous operation. Therefore, protection by Fe-treated NiO films is a promising strategy to achieve highly efficient and stable photoanodes.

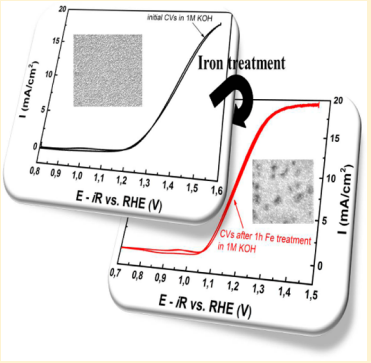

SECTION: Energy Conversion and Storage; Energy and Charge Transport

The sunlight-assisted electrolysis of water using a tandem device photoelectrochemical (PEC) cell theoretically has the potential to achieve an overall solar-to-hydrogen efficiency of about 29%.[1,2] Similar efficiencies can be obtained with a coupled photovoltaic−electrolyzer process, but the potential for low production costs of a tandem PEC cell renders it a favorable approach.[1,3] Nevertheless, there are still significant challenges in designing a highly efficient device.[2] The kinetically slow oxygen evolution reaction (OER) causes major efficiency losses, and the long-term stability of suitable semiconductors, like Si or GaAs, under highly oxidative conditions is poor. While rather complex structures can be used,[4,5] it was recently pointed out by Seger et al.[6] that anodic protection of unstable photoanodes might be possible by applying coatings of metals and their oxides. Here, the protection layer simultaneously acts as oxygen evolution catalysts. These films should be very thin due to their intrinsic high optical absorption properties. Consequently, some efforts have been made using thin films such as Ir/IrO_x[7] or MnO_x.[8] Semiconducting metal oxides constitute another class of suitable anode protection layer (APL). The requirements that the semiconductor should be p-type and that the valence band should be located cathodic of the oxygen evolution potential to allow for a hole accumulation layer limit the number of candidates.[6] Interestingly, Hu et al.[9] used a "leaky" amorphous TiO_2 film as an anodic protection layer. Although TiO_2 is well-known to be an n-type semiconductor, Hu et al. argued that they could introduce defects that permitted hole transfer. From the constraints described by Seger et al.,[6] NiO, a p-type semiconductor, appears to be an interesting candidate. It has a large band gap of 3.7 eV,[5,10−13] and the valence band is located at ∼1.0 V versus RHE.[10] In fact, Sun et al. used NiO or NiRuO on an n-Si photoanode and demonstrated the applicability of NiO as an APL; however, the photoanode assemblies suffered from a relatively poor performance.[5,11] While a severe degradation of the performance was reported with NiO over short time periods, the stability was improved by incorporation of Ru.[5,11] However, the Ru incorporation resulted in a reduced optical transmittance of the NiRuO film. Thus, the potential of highly transparent NiO thin films as an APL has not been successfully proven yet. Nevertheless, nickel oxides are widely used as OER catalysts.[9,14−17] Moreover, trace amounts of Fe incorporated into the NiO structure drastically improve the performance.[14−19] Therefore, NiO itself was concluded to be a mediocre OER catalyst, and instead, $Ni_{1-x}Fe_x$ oxyhydroxide electrocatalysts were reported to be the highly active species.[9] In alkaline electrolyte, these mixed metal OER catalysts exhibit almost an order of magnitude higher activities than noble metal electrocatalysts.[14,15]

Received: September 4, 2014
Accepted: September 24, 2014
Published: September 24, 2014

In this work, we report on the use of an inexpensive and highly transparent p-type NiO thin film as an APL for p^+−n-Si photoanodes for the PEC oxidation of water in strong alkaline conditions (pH 14). Furthermore, a NiO thin film prepared by sputter-deposition will be shown to serve as an active material for water oxidation itself. By employing a pretreatment in iron-containing KOH (10 mM Fe), the performance of the NiO-protected p^+−n-Si photoanode can be significantly improved without changing the "bulk" properties of the NiO anodic protection layer, that is, transparency and stability against corrosion. The iron-treated NiO thin film protection presented here can provide an attractive synthesis route with potentially low fabrication costs. Furthermore, the oxygen evolution performance in a highly alkaline solution achieved with these photoanode assemblies is among the best reported.

Photoanodes consisting of p^+−n-Si were prepared similar to n^+−p-Si in previous reports (for further information, see the Supporting Information (SI)).[7,20,21] Prior to the deposition of NiO films, the p^+−n-Si photoanode substrates were sputtered in Ar (20 mTorr, 50 sccm Ar, 35 W, for 2 min). Subsequently, a 5 nm Ni film was deposited in 3 mTorr of pure Ar at 140 W followed by the deposition of 50 nm of NiO in 3 mTorr at an Ar/O_2 ratio of 5:2 at 140 W. Electrochemical quartz crystal microbalance (EQCM) substrates or glass substrates were modified with NiO thin films using similar process conditions. All electrochemical measurements were performed in high-purity 1 M KOH (for further information, see the SI).

NiO thin films with a nominal thickness of 50 nm were prepared on glass substrates at different process conditions to optimize the transmittance of the obtained thin films. Independent of the process conditions used, the optical band gap of NiO was estimated to be 3.5−3.6 eV, which is in good agreement with that from previous studies on NiO thin films.[10−12,22] Due to their high crystallinity (Figure S1, SI) and good transmittance (Figure 1A), NiO thin films used for electrochemical testing were deposited by sputter-deposition at 573 K.

Scanning electron (SEM) and atomic force microscopy (AFM) showed that the morphology of a typical 50 nm NiO thin film sputtered on a Si substrate is rough (Figure S2, SI). The NiO film is typically grown with inclined orientation and a columnar grain structure with variations of up to 30 nm in height. SEM cross-sectional images coupled with energy dispersive spectroscopy (EDS) analysis (Figure S2, SI), however, indicated that the NiO film is continuous above the Si substrate, thus covering the surface completely.

NiO is well-known to be a hole-selective semiconductor.[10,22−24] To confirm the p-type semiconducting character of the sputter-deposited NiO thin film, dark electrochemical impedance measurements were performed. The resulting Mott−Schottky plot (Figure 1B) shows a negative slope, confirming the p-type behavior of the NiO films. The flat band potential (E_{FB}) and the acceptor density (N_A) were estimated to be E_{FB} = 0.99 V versus RHE and N_A = ~4.4 × 10^{19} cm^{-3}, respectively. These values are in good agreement with those from previous studies on NiO thin films.[24] Due to low current density through the film, the doping density may not be crucial for NiO films when used as protection layers and the catalytically active material on Si photoanodes. Nevertheless, this high dopant density should provide a sufficiently low series resistance.

The dark electrochemical properties of NiO thin films deposited on EQCMs were investigated by means of cyclic

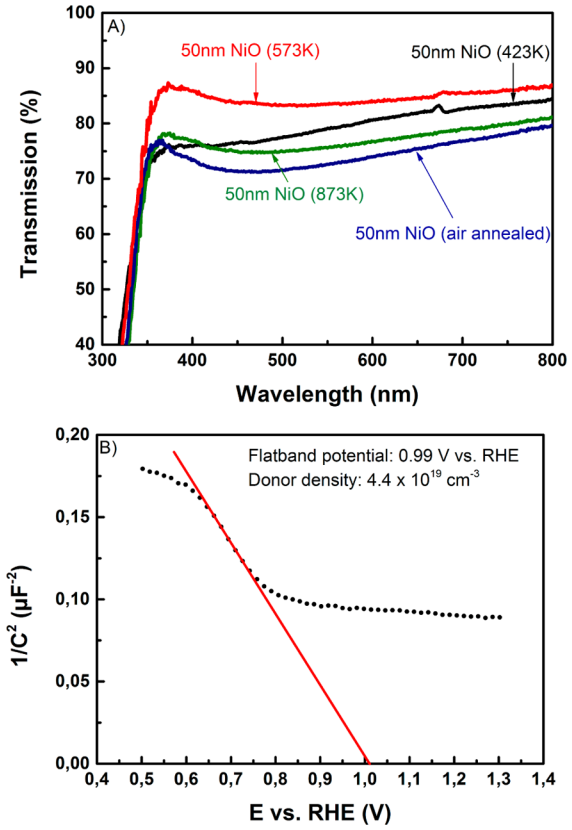

Figure 1. (A) UV−vis transmission spectra of differently prepared NiO thin films on glass substrates. (B) Mott−Schottky plot of a NiO thin film prepared at 573 K on Si substrate. The impedance measurement was performed in 1 M KOH.

voltammetry (CV), chronopotentiometry (CP), and chronoamperometry (CA) in 1 M KOH. The as-deposited NiO films show poor performance for the OER, and overpotentials of ~500 mV are required to achieve a current density of 10 mA/cm^2 (Figure 2A). However, subsequent cycling in the potential range from 0.7 to 1.7 V versus RHE revealed that the activity is increasing during cycling (Figure S3, SI). This behavior can be attributed to the incorporation of trace amounts of Fe and/or the transformation of NiO to NiOOH.[14,15] According to the Pourbaix diagram, the conversion of NiO to $Ni(OH)_2$ is possible during potential cycling in alkaline electrolyte to highly anodic potentials (>0.8 V versus SHE).[25] In order to improve the activity of NiO films further and overrule the influence of trace metal residues, Fe was intentionally added to the electrolyte. As expected,[14−16] the current increased significantly following this treatment (Figure 2A), which most likely can be attributed to a partial charge transfer from Ni to Fe.[15,26] Thus, Ni with higher oxidation power and lower overpotentials would be accessible for OER. Furthermore, an enhancement in conductivity might alter the OER performance.[15]

The EQCM results show a significant increase in mass during treatment of NiO in an Fe-containing solution (Figure 2B), which was found to level off after ~1 h of treatment. We attribute this increase in mass at least partially to Fe incorporation occurring in parallel to oxygen evolution (see the SI for further details). Furthermore, a significantly higher and relatively stable activity (current densities of 120 mA/cm^2) was achieved immediately after starting the treatment. In

dx.doi.org/10.1021/jz501872k | J. Phys. Chem. Lett. 2014, 5, 3456−3461

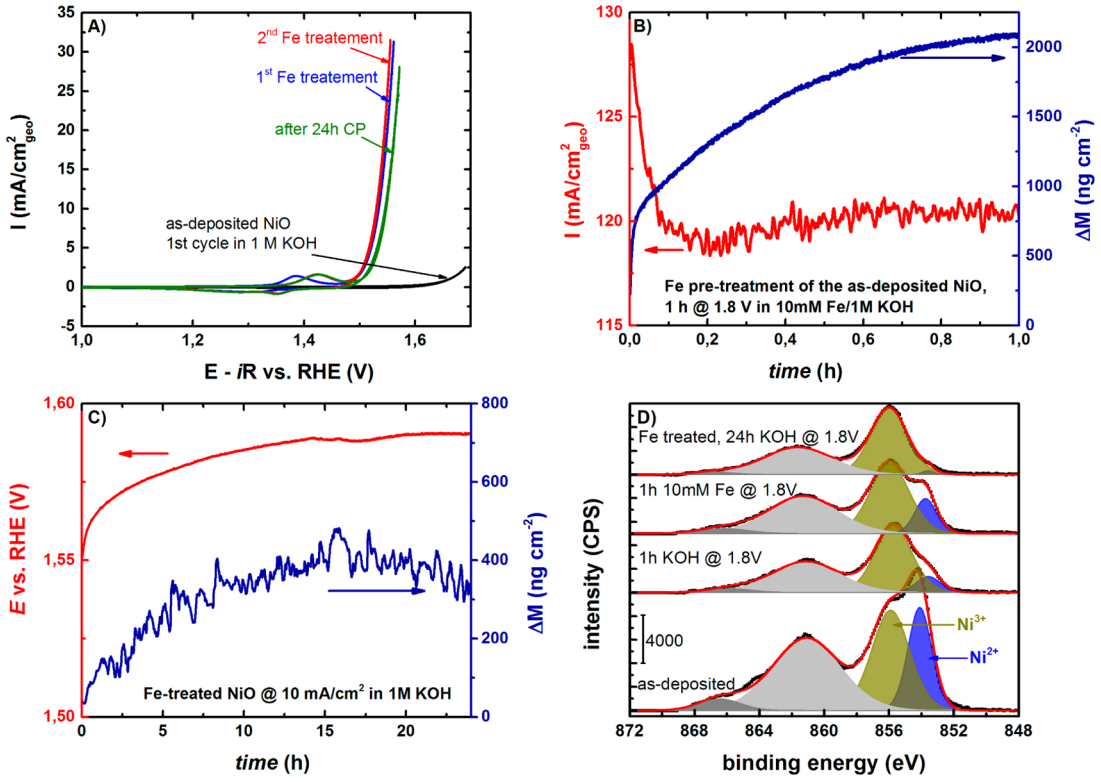

Figure 2. Dark eleochemical measurements. (A) CV curves of a NiO and Fe-treated NiO thin films on EQCM substrates. (B) CA performed with an as-deposited NiO thin film in a 10 mM Fe-containing 1 M KOH solution at 1.8 V versus RHE for 1 h. (C) CP measurement performed at a constant current density of 10 mA/cm^2 with Fe-treated NiO thin films on EQCM substrates in high-purity 1 M KOH for 24 h. (D) Ni 2p XPS spectra of NiO and Fe-treated NiO thin films after different electrochemical treatments.

contrast, only a slight increase in mass, presumably due to the conversion of NiO to NiOOH, and a decrease in current density (max. 20 mA/cm^2) with time was observed for the as-deposited NiO (Figure S4, SI). Hence, the Tafel slope (~24 mV/dec) and the OER overpotential (η = 300 mV) required to achieve meaningful current densities are significantly improved for the Fe-treated sample compared with the as-deposited NiO shown in Figure 2A. Due to the stable performance of the Fe-treated NiO thin film electrode and the rather slowly increasing mass of the film, it is reasonable to assume that the Fe incorporation into NiO is a fast process that might be limited to the first few nanometers of the NiO film. Therefore, a detailed mechanism of the iron incorporation into NiO thin films and the migration during electrochemical testing is currently under investigation. A first attempt to determine the Fe concentration by XPS failed due the unfavorable cross section of Fe and overlapping Ni Auger signals.

It was recently proposed by Frydendal et al.[27] that the most meaningful lifetime evaluation of thin films can be achieved by performing electrochemical long-term tests accompanied by inductively coupled plasma mass spectrometry (ICP-MS) to evaluate the metal content in the electrolyte due to corrosion. A long-term test was performed at a constant current density of 10 mA/cm^2 for 24 h in high-purity 1 M KOH with the Fe-pretreated NiO sample (Figure 2C), and the electrolyte was probed afterward to estimate the nickel content in solution. The chronopotentiometric measurement showed that the potential needed to maintain a stable current density of 10 mA/cm^2 was slightly increasing (25 mV) within the first 12 h of testing, whereafter the potential required to drive 10 mA/cm^2 stabilized. Accordingly, an anodic shift of the current−voltage curve was observed after the 24 h long-term test (Figure 2A). The anodic shift was found to be reversible after additional Fe-treatment (Figure 2A), suggesting Fe leaching out and equilibration with the electrolyte. This was confirmed by ICP-MS showing iron residues in the electrolyte. An additional gain of mass was observed for the Fe-treated NiO thin film during the CP measurement in high-purity 1 M KOH (no Fe) (Figure 2C). The mass increased by ~400 ng/cm^2 during the first 12 h of testing and stabilized afterward, thus following the same trend as the chronopotentiometric test (Figure 2C). Even though the mass increased, the ICP-MS results showed that ~16 ng of Ni dissolved away from the 1.37 cm^2 EQCM electrode. Because results indicate that Fe is lost due to solution equilibration and Ni is lost due to corrosion, we attribute the mass increase to a further oxidation of the NiO film. Indeed, characterization of the surfaces of different NiO samples by XPS showed that NiO is gradually oxidized during prolonged measurements (Figure 2D). With a mass loss of ~12 ng Ni/(cm^2 day), 0.06 monolayers (ML) of NiO would be lost every 24 h of continuous operation. In other words, the 50 nm NiO film would require ~2800 days or 7.6 years of continuous operation to fully corrode, based on extrapolation from the 24 h test. In a comparative CA measurement at 1.8 V versus RHE, a loss of 0.077 ML NiO/day was observed, giving an expected lifetime of ~2200 days for a 50 nm film. Thus, Fe-treated NiO appears to be highly stable. We note that a real water splitting device will only be evolving O_2 for a part of the day. Thus, the durability numbers that we present are conservative estimates of how long the NiO can function as a protection layer even though a certain thickness of NiO thin films is certainly

dx.doi.org/10.1021/jz501872k | J. Phys. Chem. Lett. 2014, 5, 3456−3461

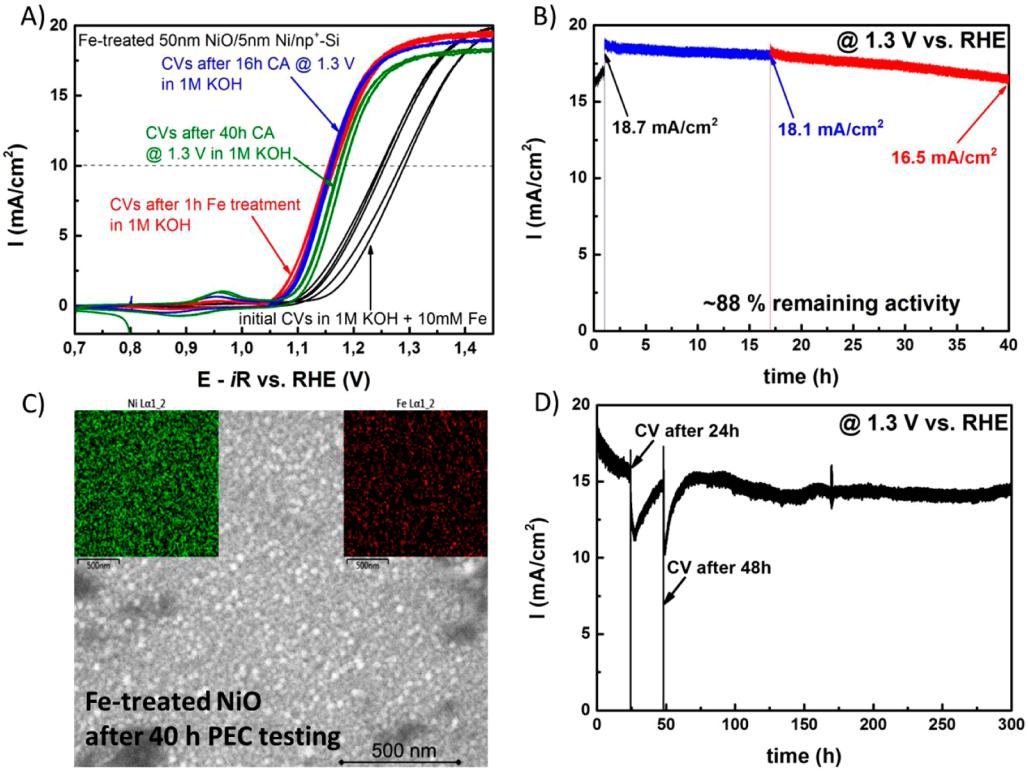

Figure 3. (A) CV curves of PEC measurements of Fe-treated NiO thin films on p^+−n-Si photoanodes after various treatments. (B) Corresponding CA measurement performed with an Fe-treated NiO thin film at 1.3 V versus RHE for 40 h. (C) SEM picture with the Ni and Fe distribution mapped by EDS of the Fe-treated NiO thin film after 40 h of chronoamperometric testing at 1.3 V versus RHE. (D) The 300 h long-term CA testing of an Fe-treated NiO-protected p^+−n-Si photoanode at 1.3 V versus RHE. All PEC measurements were performed in 1 M KOH under 38.6 mW/cm^2 of simulated sunlight (AM 1.5G, filtered $\lambda > 635$ nm).

required to chemically protect the underlying Si (for further information, see the SI).

Subsequently, PEC measurements were performed with NiO/p^+−n-Si and Fe-treated NiO/p^+−n-Si photoanodes to evaluate their applicability in a tandem device that consists of a large band gap photocathode and a small band gap photoanode. In this design, the photoanode could consist of Si, which has an almost optimal band gap (for the small band gap semiconductor) for highly efficient tandem device PEC cells.[28] As expected, the as-deposited pure NiO/p^+−n-Si photoanodes show poor performance for oxygen evolution. An applied potential of 1.4 V versus RHE is required to obtain a current density of 10 mA/cm^2 (Figure S5, SI), which is due to a poor Tafel slope (~170 mV/dec).

Accordingly, during CA measurements at 1.3 V versus RHE, a maximum current density of 3.5 mA/cm^2 was obtained (Figure S6, SI). The initial decay in the CA measurement could be attributed to the contamination of the electrode, presumably by potassium ions, whereas the slow increase with prolonged irradiation could be due to incorporation of small amounts of Fe present in the electrolyte. Indeed, the CV curve is slowly shifting cathodically, indicating the incorporation of Fe into the NiO film (Figure S5, SI).

The Fe pretreatment was subsequently performed by irradiating the as-deposited NiO/p^+−n-Si photoanodes at 1.3 V versus RHE with 38.6 mW/cm^2 of simulated sunlight ($\lambda >$ 635 nm, AM 1.5G) to match the conditions in a tandem device. The p^+−n-Si photoanodes are known to give a photovoltage of ~500 mV;[7] therefore, these conditions were chosen to obtain comparable treatments with the dark experiments (i.e., 1.3 V versus RHE + 500 mV = 1.8 V versus RHE). The CV (Figure 3A) curve obtained in the 10 mM Fe-containing 1 M KOH electrolyte before 1 h of treatment, as well as the CV curve immediately after Fe treatment in high-purity 1 M KOH, indicates that the photocurrent onset is already shifted cathodically by immersing the electrode in the Fe-containing electrolyte, but the main improvement takes place over 1 h of treatment. Furthermore, it should be noticed that saturation currents similar to the as-deposited NiO/p^+−n-Si photoanodes were obtained, indicating a high transparency of the films even after Fe treatment. Thus, after 1 h of treatment, 10 mA/cm^2 was achieved at an applied potential of 1.15 V versus RHE, making it an almost perfect match for a well-protected PbI_2-based perovskite photocathode. This is a significantly improved result for the NiO-catalyzed OER over those reported by Hu et al.[9] and Kenney et al.[17] as an applied potential of 1.23 V versus RHE was usually required to obtain current densities of 10 mA/cm^2 with their photoanodes. It is important to point out that in our experiment, only the red part of the solar spectrum (38.6 mW/cm^2 of simulated sunlight $\lambda >$ 635 nm, AM 1.5G) was used, whereas using the full spectrum (and even higher light intensities) as done by Hu et al.[9] and Kenney et al.[17] would have further improved the performance because increased light intensity increases the photovoltage. Even Ir-catalyzed Si-based photoanodes showed worse performance.[29] Thus, to the best of our knowledge, this functionalization results in the highest photoelectrocatalytic OER performance for a Si-based photoanode in alkaline electrolyte yet.

During 40 h of CA testing at 1.3 V versus RHE, the electrode was relatively stable, and a decrease of only 12% over the

dx.doi.org/10.1021/jz501872k | J. Phys. Chem. Lett. 2014, 5, 3456−3461

extended time period was observed (Figure 3B). The decrease was due to a lower saturation current, most likely caused by adventitious contamination, which was also observed for the as-deposited NiO/p^+−n-Si photoanode (Figure S5, SI). Simply rinsing the electrode surface with distilled water recovered the initial saturation current. Additionally, after 40 h, the photocurrent onset was anodically shifted by 20 mV. This shift is in good agreement with the observed shift in dark electrochemical measurements, and therefore, most likely, the initial activity can be recovered by additional Fe treatment. Comparing the SEM images of the as-deposited NiO (Figure S2, SI) with the Fe-treated NiO (Figure S7, SI) reveals that the surface of the latter is less rough. However, there are no obvious changes in the film morphology of the 40 h tested Fe-treated NiO compared to the 1 h tested Fe-treated NiO material.

Finally, a Fe-treated NiO/p^+−n-Si was subjected to a 300 h stability test at 1.3 V versus RHE (Figure 3D). In-between CVs were taken after 24 and 48 h of operation. While there are no differences in the iron pretreatment for the photoanodes subjected to the 40 h (Figure 3B) and the 300 h (Figure 3D) CA long-term tests, some variations in the performance were observed. Generally, the behavior of the 300 h tested Fe-treated NiO/p^+−n-Si was similar to that of the 40 h test, but a sharp decay and a slow recovery of the performance was observed for the 300 h tested sample after taking a CV (Figure 3D). However, a stable photocurrent of 14.5 mA/cm^2 was observed when the sample was continuously operated at 1.3 V versus RHE for 5 additional days. The decrease in current was most likely due to contamination. Furthermore, the current−voltage curves indicate that a larger fraction of Ni atoms participate in the $Ni^{2+/3+}$ redox wave (Figure S8, SI) at peak potentials at 0.98 and 0.92 V versus RHE in the anodic and cathodic sweeps, respectively. Thus, aging of the films appears to occur over a relatively long time scale, and the implications for stability should be further explored.

In conclusion, we have demonstrated that Fe-treated NiO thin films are suitable, highly transparent protection layers for p^+−n-Si photoanodes enabling OER at low overpotentials. This was shown by a combination of electrochemical measurements and various characterization techniques. According to Ni dissolution rates measured for dark electrochemical oxygen evolution, an expected lifetime of more than 2000 days can, in principle, be achieved with a 50 nm thick Fe-treated NiO film. Utilizing these Fe-treated NiO films to protect p^+−n-Si photoanodes, current densities of 10 mA/cm^2, which is the requirement for a >10% efficient tandem device, could be achieved at an applied potential of 1.15 V versus RHE. A stable performance for at least 300 h was obtained with these devices. Furthermore, the Fe-treated NiO/p^+−n-Si assembly reported herein is among the best-performing Si-based photoanodes in the literature. The presented Fe-treated NiO thin films might additionally be a suitable protective layer for large band gap photoanodes. Future studies will aim to understand the photoanode assembly in greater detail, particularly the Fe incorporation into the NiO structure and its influence on the long-term stability.

■ ASSOCIATED CONTENT

Supporting Information

Experimental details, further electrochemical characterization, and further characterization by XRD, SEM, and AFM measurements. This material is available free of charge via the Internet at http://pubs.acs.org.

■ AUTHOR INFORMATION

Corresponding Author

*E-mail: ibchork@fysik.dtu.dk.

Author Contributions

§B.M., A.A.P., and R.F. contributed equally to the manuscript.

Notes

The authors declare no competing financial interest.

■ ACKNOWLEDGMENTS

B.M. acknowledges funding from the Ruhr-University Research School Plus throughout the Gateway Fellowship Initiative. For further funding, we gratefully acknowledge the Danish Ministry of Science's UNIK initiative Catalysis for Sustainable Energy (CASE), the Danish National Research Foundation's Center for Individual Nanoparticle Functionality (DNRF54), and the Danish Council for Strategic Research's project MEDLYS (10-093906). We thank K. Nielsen for support with XPS measurements.

■ REFERENCES

(1) McKone, J. R.; Lewis, N. S.; Gray, H. B. Will Solar-Driven Water-Splitting Devices See the Light of Day? *Chem. Mater.* **2014**, *26*, 407−414.

(2) Walter, M. G.; Warren, E. L.; McKone, J. R.; Boettcher, S. W.; Mi, Q.; Santori, E. A.; Lewis, N. S. Solar Water Splitting Cells. *Chem. Rev.* **2010**, *110*, 6446−6473.

(3) Pinaud, B. A.; Benck, J. D.; Seitz, L. C.; Forman, A. J.; Chen, Z.; Deutsch, T. G.; James, B. D.; Baum, K. N.; Baum, G. N.; Ardo, S.; et al. Technical and Economic Feasibility of Centralized Facilities for Solar Hydrogen Production via Photocatalysis and Photoelectrochemistry. *Energy Environ. Sci.* **2013**, *6*, 1983.

(4) Cox, C. R.; Winkler, M. T.; Pijpers, J. J. H.; Buonassisi, T.; Nocera, D. G. Interfaces between Water Splitting Catalysts and Buried Silicon Junctions. *Energy Environ. Sci.* **2013**, *6*, 532.

(5) Sun, K.; Park, N.; Sun, Z.; Zhou, J.; Wang, J.; Pang, X.; Shen, S.; Noh, S. Y.; Jing, Y.; Jin, S.; et al. Nickel Oxide Functionalized Silicon for Efficient Photo-Oxidation of Water. *Energy Environ. Sci.* **2012**, *5*, 7872.

(6) Seger, B.; Castelli, I. E.; Vesborg, P. C. K.; Jacobsen, K. W.; Hansen, O.; Chorkendorff, I. 2-Photon Tandem Device for Water Splitting: Comparing Photocathode First versus Photoanode First Designs. *Energy Environ. Sci.* **2014**, *7*, 2397.

(7) Mei, B.; Seger, B.; Pedersen, T.; Malizia, M.; Hansen, O.; Chorkendorff, I.; Vesborg, P. C. K. Protection of p^+-n-Si Photoanodes by Sputter-Deposited Ir/IrO_x Thin Films. *J. Phys. Chem. Lett.* **2014**, *5*, 1948−1952.

(8) Strandwitz, N. C.; Comstock, D. J.; Grimm, R. L.; Nichols-Nielander, A. C.; Elam, J.; Lewis, N. S. Photoelectrochemical Behavior of n-Type Si(100) Electrodes Coated with Thin Films of Manganese Oxide Grown by Atomic Layer Deposition. *J. Phys. Chem. C* **2013**, *117*, 4931−4936.

(9) Hu, S.; Shaner, M. R.; Beardslee, J. A.; Lichterman, M.; Brunschwig, B. S.; Lewis, N. S. Amorphous TiO_2 Coatings Stabilize Si, GaAs, and GaP Photoanodes for Efficient Water Oxidation. *Science* **2014**, *344*, 1005−1009.

(10) Bai, S.; Cao, M.; Jin, Y.; Dai, X.; Liang, X.; Ye, Z.; Li, M.; Cheng, J.; Xiao, X.; Wu, Z.; et al. Low-Temperature Combustion-Synthesized Nickel Oxide Thin Films as Hole-Transport Interlayers for Solution-Processed Optoelectronic Devices. *Adv. Energy Mater.* **2014**, *4*, 1301460.

(11) Sun, K.; Pang, X.; Shen, S.; Qian, X.; Cheung, J. S.; Wang, D. Metal Oxide Composite Enabled Nanotextured Si Photoanode for

Efficient Solar Driven Water Oxidation. *Nano Lett.* **2013**, *13*, 2064−2072.
(12) Trotochaud, L.; Mills, T. J.; Boettcher, S. W. An Optocatalytic Model for Semiconductor−Catalyst Water-Splitting Photoelectrodes Based on In Situ Optical Measurements on Operational Catalysts. *J. Phys. Chem. Lett.* **2013**, *4*, 931−935.
(13) Miller, E. L. Electrochemical and Electrochromic Behavior of Reactively Sputtered Nickel Oxide. *J. Electrochem. Soc.* **1997**, *144*, 1995.
(14) Trotochaud, L.; Ranney, J. K.; Williams, K. N.; Boettcher, S. W. Solution-Cast Metal Oxide Thin Film Electrocatalysts for Oxygen Evolution. *J. Am. Chem. Soc.* **2012**, *134*, 17253−17261.
(15) Trotochaud, L.; Young, S. L.; Ranney, J. K.; Boettcher, S. W. Nickel−Iron Oxyhydroxide Oxygen-Evolution Electrocatalysts: The Role of Intentional and Incidental Iron Incorporation. *J. Am. Chem. Soc.* **2014**, *136*, 6744−6753.
(16) McCrory, C. C. L.; Jung, S.; Peters, J. C.; Jaramillo, T. F. Benchmarking Heterogeneous Electrocatalysts for the Oxygen Evolution Reaction. *J. Am. Chem. Soc.* **2013**, *135*, 16977−16987.
(17) Kenney, M. J.; Gong, M.; Li, Y.; Wu, J. Z.; Feng, J.; Lanza, M.; Dai, H. High-Performance Silicon Photoanodes Passivated with Ultrathin Nickel Films for Water Oxidation. *Science* **2013**, *342*, 836−840.
(18) Louie, M. W.; Bell, A. T. An Investigation of Thin-Film Ni−Fe Oxide Catalysts for the Electrochemical Evolution of Oxygen. *J. Am. Chem. Soc.* **2013**, *135*, 12329−12337.
(19) Song, F.; Hu, X. Exfoliation of Layered Double Hydroxides for Enhanced Oxygen Evolution Catalysis. *Nat. Commun.* **2014**, *5*, 1−9.
(20) Seger, B.; Pedersen, T.; Laursen, A. B.; Vesborg, P. C. K.; Hansen, O.; Chorkendorff, I. Using TiO_2 as a Conductive Protective Layer for Photocathodic H_2 Evolution. *J. Am. Chem. Soc.* **2013**, *135*, 1057−1064.
(21) Seger, B.; Laursen, A. B.; Vesborg, P. C. K.; Pedersen, T.; Hansen, O.; Dahl, S.; Chorkendorff, I. Hydrogen Production Using a Molybdenum Sulfide Catalyst on a Titanium-Protected n^+p-Silicon Photocathode. *Angew. Chem., Int. Ed.* **2012**, *51*, 9128−9131.
(22) Irwin, M. D.; Buchholz, D. B.; Hains, A. W.; Chang, R. P. H.; Marks, T. J. p-Type Semiconducting Nickel Oxide as an Efficiency-Enhancing Anode Interfacial Layer in Polymer Bulk-Heterojunction Solar Cells. *Proc. Natl. Acad. Sci. U.S.A.* **2008**, *105*, 2783−2787.
(23) Xiong, D.; Xu, Z.; Zeng, X.; Zhang, W.; Chen, W.; Xu, X.; Wang, M.; Cheng, Y.-B. Hydrothermal Synthesis of Ultrasmall $CuCrO_2$ Nanocrystal Alternatives to NiO Nanoparticles in Efficient p-Type Dye-Sensitized Solar Cells. *J. Mater. Chem.* **2012**, *22*, 24760.
(24) Chan, X.-H.; Robert Jennings, J.; Anower Hossain, M.; Koh Zhen, Yu. K.; Wang, Q. Characteristics of p-NiO Thin Films Prepared by Spray Pyrolysis and Their Application in CdS-Sensitized Photocathodes. *J. Electrochem. Soc.* **2011**, *158*, H733.
(25) Beverskog, B.; Puigdomenech, I. Revised Pourbaix Diagrams for Nickel at 25−300 °C. *Corros. Sci.* **1997**, *39*, 969−980.
(26) Yeo, B. S.; Bell, A. T. In Situ Raman Study of Nickel Oxide and Gold-Supported Nickel Oxide Catalysts for the Electrochemical Evolution of Oxygen. *J. Phys. Chem. C* **2012**, *116*, 8394−8400.
(27) Frydendal, R.; Paoli, E. A.; Knudsen, B. P.; Wickman, B.; Malacrida, P.; Stephens, I. E.L.; Chorkendorff, I. Benchmarking the Stability of Oxygen Evolution Reaction Catalysts: The Importance of Monitoring Mass Losses. *ChemElectroChem* **2014**, DOI: 10.1002/celc.201402262.
(28) Laursen, A. B.; Kegnæs, S.; Dahl, S.; Chorkendorff, I. Molybdenum Sulfides—Efficient and Viable Materials for Electro- and Photoelectrocatalytic Hydrogen Evolution. *Energy Environ. Sci.* **2012**, *5*, 5577.
(29) Chen, Y. W.; Prange, J. D.; Dühnen, S.; Park, Y.; Gunji, M.; Chidsey, C. E. D.; McIntyre, P. C. Atomic Layer-Deposited Tunnel Oxide Stabilizes Silicon Photoanodes for Water Oxidation. *Nat. Mater.* **2011**, *10*, 539−544.